HHS Public Access

Author manuscript

Clin Neurophysiol. Author manuscript; available in PMC 2021 December 01.

Published in final edited form as:

Clin Neurophysiol. 2020 December ; 131(12): 2781–2792. doi:10.1016/j.clinph.2020.09.010.

Effects of depth electrode montage and single-pulse electrical stimulation sites on neuronal responses and effective connectivity

Takumi Mitsuhashi[1,5,*], **Masaki Sonoda**[1,6,*], **Hirotaka Iwaki**[1,7], **Aimee F. Luat**[1,2], **Sandeep Sood**[3], **Eishi Asano**[1,2,4,*]

[1]Department of Pediatrics, Children's Hospital of Michigan, Detroit Medical Center, Wayne State University, Detroit, MI 48201, USA

[2]Department of Neurology, Children's Hospital of Michigan, Detroit Medical Center, Wayne State University, Detroit, MI 48201, USA

[3]Department of Neurosurgery, Children's Hospital of Michigan, Detroit Medical Center, Wayne State University, Detroit, MI 48201, USA

[4]Translational Neuroscience Program, Wayne State University, Detroit, MI 48202, USA

[5]Department of Neurosurgery, Juntendo University, Tokyo, 1138421, Japan

[6]Department of Neurosurgery, Yokohama City University, Yokohama, 2360004, Japan

[7]Department of Epileptology, Tohoku University Graduate School of Medicine, Sendai, 9808575, Japan

Abstract

Objective: To determine the optimal depth electrode montages for the assessment of effective connectivity based on single-pulse electrical stimulation (SPES). To determine the effect of SPES locations on the extent of resulting neuronal propagations.

Methods: We studied 14 epilepsy patients who underwent invasive monitoring with depth electrodes and measurement of cortico-cortical evoked potentials (CCEPs) and cortico-cortical spectral responses (CCSRs). We determined the effects of electrode montage and stimulus sites on the CCEP/CCSR amplitudes.

Results: Bipolar and Laplacian montages effectively reduced the degree of SPES-related signal deflections at extra-cortical levels, including outside the brain, while maintaining those at the

Corresponding Author: Eishi Asano MD, PhD, Division of Pediatric Neurology, Children's Hospital of Michigan, Wayne State University, 3901 Beaubien St., Detroit, MI 48201, USA, Phone: +1-313-745-5547, Fax: +1-313-745-9435, easano@med.wayne.edu.
*Equal contribution.

Disclosure

None of the authors have potential conflicts of interest to be disclosed.

cortical level. SPES of structures more proximal to the deep white matter, compared to the cortical surface, elicited greater CCEPs and CCSRs.

Conclusions: On depth electrode recording, bipolar and Laplacian montages are suitable for measurement of near-field CCEPs and CCSRs. SPES of the white matter axons may induce neuronal propagations to extensive regions of the cerebral cortex.

Significance: This study helps to establish the practical guidelines on the diagnostic use of CCEPs/CCSRs.

Keywords

pediatric epilepsy surgery; video EEG monitoring; electrocorticography (ECoG); stereo-electroencephalography (sEEG); effective connectivity; functional brain mapping; intracranial recording

1. Introduction

Invasive presurgical evaluation for patients with drug-resistant epilepsy includes the assessment of inter-regional effective connectivity, as rated by the extent of neuronal propagations induced by single-pulse electrical stimulation (SPES) via subdural or depth electrodes (Matsumoto et al., 2017). The magnitude of sharply-contoured neuronal responses to SPES is commonly quantified with cortico-cortical evoked potentials (CCEPs) and cortico-cortical spectral responses (CCSRs) with a latency of 11-50 ms (Matsumoto et al., 2004; Alarcón et al., 2012; Matsuzaki et al., 2013; Gkogkidis et al., 2017; Usami et al., 2019; Sugiura et al., 2020). Cortical sites showing such early near-field CCEP/CCSR components are inferred to have single-axonal effective connectivity from the SPES site (Matsumoto et al., 2007; Silverstein et al., 2020). Thereby, higher CCEP/CCSR magnitudes indicate more robust interregional effective connectivity (Silverstein et al., 2020). Many SPES studies suggest that early, near-field CCEP/CCSR components are useful to localize the eloquent pathways (Matsumoto et al., 2004; 2017; Nishida et al., 2017; Trebaul et al., 2018; Sugiura et al., 2020). Conversely, late CCEP/CCSR components with a latency of >100 ms may reflect either post-excitatory inhibitory responses, indirect responses via a cortico-thalamo-cortical propagation, or a mixture of both (Logothetis et al., 2010; van 't Klooster et al., 2011; Alarcón et al., 2012; Matsumoto et al., 2017). A study reported that SPES of the seizure onset zone (SOZ) elicited an early CCEP within 50 ms, deemed to be a physiological response, which was followed by a delayed high-frequency activity mimicking an interictal epileptiform discharge (van 't Klooster et al., 2011). The present study, while focusing on the early CCEP/CCSR components recorded on depth electrodes, determined the optimal analytic approach suitable for the assessment of inter-regional effective connectivity.

What electrode montage should be used for the clinical assessment of CCEPs and CCSRs recorded on depth electrodes? Using our empirical CCEPs and CCSRs recorded on stereo-electroencephalography (sEEG), we demonstrated what electrode montage is suitable to measure a near-field potential generated by a local cortical tissue receiving an SPES-induced propagation signal. We thereby assumed that the cerebral cortex is the source of CCEPs/

CCSRs, whereas the structures outside the brain do not generate CCEPs/CCSRs. We defined a suitable montage as that on which CCEP/CCSR amplitudes are minimized at extra-cortical channels, particularly those outside the brain (Fig. 1). We tested the hypothesis that, on depth electrode recording, bipolar and Laplacian montages would be more suitable than common average reference montage (denoted as 'average montage' below). Bipolar and Laplacian montages were suggested to effectively eliminate the influence of electrical activities taking place at distant sources (also known as far-field potentials; Lachaux et al., 2003; Worrell et al., 2012; Tenke and Kayser, 2012).

We then tested the hypothesis that SPES of white matter channels, compared to gray matter ones, would elicit CCEPs/CCSRs at more extensive regions. We also tested another hypothesis that cortical SPES via depth electrodes, compared to that via subdural electrodes, would likewise elicit CCEPs/CCSRs more extensively. The present study should be able to address these hypotheses since given depth electrodes typically sampled both cortex and white matter, and we employed the same stimulus intensity and pulse width within and across patients. A previous sEEG study reported that subcortical SPES elicited CCEPs with a 61% higher probability compared to cortical SPES (Trebaul et al., 2018). We expected that our CCEP/CCSR data recorded with sEEG electrodes, as well as those measured with a combination of depth and subdural disk electrodes, would provide the observations consistent with that reported in Trebaul et al., 2018.

2. Methods

2.1. Participants

The inclusion criteria included: (a) extraoperative intracranial electroencephalography (iEEG) recording at Children's Hospital of Michigan in Detroit between February 2013 and January 2019, (b) usage of depth electrodes, and (c) assessment of SPES-based effective connectivity. We performed all procedures as part of our routine presurgical evaluation, and the spatial extent and duration of iEEG recording and electrical stimulation were determined based on clinical demands (Asano et al., 2009; Matsumoto et al., 2017; Kambara et al., 2018; Silverstein et al., 2020). The Wayne State University Institutional Review Board has approved the present study. We obtained written informed consent from the legal parents or guardians of patients. We likewise received written assent from children older than 13, and oral assent from younger children.

2.2. Intracranial electrode placement

We placed intracranial electrodes for subsequent localization of the boundaries between the presumed epileptogenic zone and eloquent pathways using extraoperative iEEG recording, SPES-related neuronal responses, and electrical stimulation mapping (Nakai et al., 2017; Kambara et al., 2018; Silverstein et al., 2020; Sugiura et al., 2020). A total of three patients (patients #1 - #3 in Table 1) underwent bilateral sEEG recording; these patients had multicontact depth platinum electrodes implanted stereotactically under MRI guidance in both hemispheres. An anchor bolt tightly secured each sEEG depth electrode and minimized movement-related artifacts. Each depth electrode had eight, 12, and 16 contacts (length: 2 mm; center-to-center distance: 3.5, 3.5, and 4.43 mm, respectively; PMT, Chanhassen, MN,

USA). The remaining 11 patients underwent an open craniotomy and had implantation of a combination of subdural (3 mm exposed diameter, 10 mm center-to-center distance) and depth electrodes (six to eight contacts; length: 5 and 2 mm; center-to-center distance: 10 and 5 mm, respectively; PMT, Chanhassen, MN, USA) placed on the affected hemisphere.

2.3. Imaging process

We acquired a presurgical T1-weighted spoiled gradient-recalled echo sequence MRI and a post-implant CT image and created a fusion image accurately registering intracranial electrodes with the brain (Nakai et al., 2017; Stolk et al., 2018). Based on the assessment on coronal, axial, and sagittal fusion images, a given depth contact was classified into one of the following anatomical categories (Fig. 1): (a) deep white matter (white matter deeper than the bottoms of two adjacent sulci), (b) shallow white matter (white matter more superficial than the bottoms of two adjacent sulci), (c) gray matter (i.e., cerebral cortex), (d) cerebrospinal fluid (CSF) space (i.e., ventricle and subarachnoid space), and (e) outside the arachnoid surface of the brain. Two board-certified clinicians (a neurosurgeon [T.M.] and a neurosurgeon/epileptologist [M.S.]) independently classified depth electrode channels based on the anatomical locations. Inter-observer variability was measured using Cohen's kappa statistic (Cohen, 1960). We later achieved a consensus on the anatomical classification following group discussions. We treated all subdural electrodes as gray matter channels.

2.4. iEEG recording

We continuously acquired iEEG data at the bedside with a sampling rate of 1,000 Hz and amplifier bandpass at 0.016 - 300 Hz, using a Neurofax 1100A Digital System (Nihon Kohden America Inc., Foothill Ranch, CA, USA). The original reference was the averaged voltage of a pair of white matter contacts for sEEG recording and a pair of nonepileptic contacts for subdural iEEG recording. Such an original reference is often referred to as a system reference (Lesser et al., 2010; Nariai et al., 2011). We clinically assessed iEEG signals using average montage (Crone et al., 2001) as well as bipolar montage (Zijlmans et al., 2011; Isnard et al., 2018; Shimamoto et al., 2018). We excluded SPES-induced neuronal responses recorded at SOZ, irritative zone, or artifactual channels from further analyses of the present study. We defined the irritative zone as regions showing interictal spike discharges (Asano et al., 2009; Kural et al., 2020). Neuronal responses recorded at contacts within <1 cm from the stimulus site were also excluded from analysis (Sugiura et al., 2020; Prime et al., 2020b).

2.5. The protocol of single-pulse electrical stimulation (SPES)

We performed SPES using the method previously described (Silverstein et al., 2020; Sugiura et al., 2020). Each patient was given Fosphenytoin intravenously before initiating the SPES session. During resting sleep state, in each SPES trial, we delivered a train of electrical stimuli to a contiguous pair of depth or subdural electrodes at a frequency of 1 Hz for 40 s during a resting period of sleep. We routinely stimulate all electrode contacts placed within the brain (Cuello Oderiz et al., 2019). Each electrical stimulus consisted of a square wave pulse of 0.3 ms duration, 5 mA intensity, and biphasic polarity. The stimulus intensity was smaller than those previously reported to be safe (Valentín et al., 2002; Matsumoto et al.,

2004; Koubeissi et al., 2012; Crowther et al., 2019). None of the patients showed or reported adverse events related to the SPES procedures.

2.6. Selection of electrode montage for assessment of SPES-related neuronal propagations

We determined the effects of electrode montage on the magnitude of neuronal responses recorded at sites receiving SPES-related neuronal propagations. We re-referenced iEEG signals using EEGLAB v2019.1 (Delorme and Makeig, 2004) and analyzed neuronal responses to SPES using the four different montages. [Bilateral average montage] The reference consisted of the average of iEEG signals of all channels in both hemispheres. We computed the average reference voltage by excluding all of the iEEG signals at SOZ, irritative zone, and artifactual channels (Asano et al., 2009), those outside the brain (Isnard et al., 2018), as well as those within 3 cm from the midpoint of the SPES sites (Swann et al., 2012; Shimada et al., 2017). [Ipsilateral average montage] The reference consisted of the average of iEEG signals of all channels in the hemisphere ipsilateral to the one recording a given SPES-related neuronal response. [Bipolar montage] Each electrode was referenced to the adjacent electrode on a deeper side. [Laplacian montage] Each electrode was referenced to the average of adjacent electrodes on both sides (Mercier et al., 2017; Li et al., 2018).

2.7. Quantification of direct effective connectivity using early $CCEP_{4\text{-}60\ Hz}$

We employed a root mean square (RMS) analysis (Prime et al., 2020a) to quantify the amplitude of CCEPs on each electrode montage. We averaged iEEG signals time-locked to SPES onset, across 40 stimuli, with a time window of −200 to +800 ms with a low-frequency filter of 4.0 Hz and a high-frequency filter of 60 Hz. We computed the square root of the mean of the squares of amplitude values from 11 to 50 ms (1-ms slide) at each channel. This analytic approach was designed to measure the magnitude of early SPES-related response, also known as N1 (Matsumoto et al., 2004). We excluded the initial 10 ms period from analysis to reduce the effect of stimulus artifact on iEEG (Swann et al., 2012). With visual assessment, we confirmed the reproducibility of CCEPs at given channels.

On bipolar montage, we computed the RMS at an electrode N as the mean of RMS at N−1/N pair and N/N+1 pair. We regarded the RMS value as a CCEP amplitude below.

2.8. Quantification of direct effective connectivity using early $CCSR_{4\text{-}60\ Hz}$

We quantified the magnitude of the neuronal response to SPES using a time-frequency analysis similar to that reported previously (Tallon-Baudry et al., 1997; Oostenveld et al., 2011; Sugiura et al., 2020). The Morlet wavelet method, as implemented in the FieldTrip (http://www.fieldtriptoolbox.org), transformed iEEG voltage signals into time-frequency bins (2 Hz frequency bins; three cycles for each frequency) sliding in 1 ms steps at a time window of 11-50 ms with a bandpass of 4-60 Hz. We previously reported that this analytic time window and spectral frequency band were minimally affected by the effect of SPES-related artifacts (Sugiura et al., 2020). We defined a CCSR amplitude as the square root of the power averaged across 40 stimuli. We also computed the percent change of CCSR amplitude relative to that during the 50-200 ms pre-stimulus baseline period (Nakai et al., 2017; Sugiura et al., 2020). The cluster-based permutation test determined whether a given

channel showed a significantly reproducible CCSR amplitude augmentation (Maris and Oostenveld, 2007).

2.9. Assessment of the validity of CCSRs recorded on bilateral and ipsilateral average montages

The goal of this analysis was to determine whether bilateral or ipsilateral average montages would be unsuitable for the measurement of near-field SPES-related responses in patients who underwent bilateral depth electrode placement. We deemed an electrode montage unsuitable if a large proportion of channels outside the brain showed significantly reproducible iEEG signal deflections at an 11-50 ms latency.

2.10. Assessment of the validity of CCSRs recorded on average, bipolar, and Laplacian montages

The goal of this analysis was to test the hypothesis that bipolar montage, compared to average montage, is more suitable for measurement of near-field CCSRs in patients undergoing bilateral depth recording. We assumed that near-field CCSRs could be measured at channels proximal to a cortical generator but should be absent or markedly attenuated outside the brain with the optimal electrode montage and amplitude threshold employed. We determined what ***amplitude-based threshold (%)*** (e.g., at least 80% amplitude increase compared to the baseline) should be implemented, in addition to the cluster-based permutation test, for defining a significant CCSR. We also determined whether consideration of montage-dependent changes in CCSR amplitudes would further improve the definition of a significant CCSR. Investigators previously suggested that a far-field potential from a common distant source should be canceled out on bipolar montage (Lachaux et al., 2003; Worrell et al., 2012; Tenke and Kayser, 2012). Thus, we hypothesized that contacts outside the brain, compared to those within the cortex, would have a smaller ***bipolar-to-average amplitude ratio (%)***, defined as [CCSR amplitude on bipolar montage × 100%] divided by [CCSR amplitude on average montage]. We determined the optimal combination of 'amplitude-based threshold' and 'bipolar-to-average amplitude ratio' that minimized an unwanted observation of significant CCSRs at contacts outside the brain.

Likewise, we tested the hypothesis that Laplacian montage, compared to average montage, would be more suitable for the measurement of near-field CCSRs in patients undergoing bilateral depth recording.

2.11. The similarity of spatial profiles of CCEPs/CCSRs among different electrode montages

The Spearman's correlation tested the hypothesis that the rank order of CCEP amplitudes across contacts would be very similar between bipolar and Laplacian montages but not necessarily between average and bipolar montages. Likewise, we determined how similar the rank order of CCSR amplitudes was among different montages.

2.12. Assessment of the effect of SPES locations on the extent of resulting neuronal propagations

We tested the hypothesis that SPES of structures more proximal to the deep white matter, compared to the cortical surface, would elicit larger CCEPs and CCSRs. We employed a mixed model analysis, in which the amplitude of CCEP/CCSR was treated as a dependent variable. Fixed effect predictors included (a) the number of SPES electrodes at deep white matter (range: 0 to 2), (b) that at shallow white matter (range: 0 to 2), (c) that at gray matter (range: 0 to 2), (d) the recording hemisphere (1 if contralateral and 0 if ipsilateral to SPES), and (e) the type of recording contacts (1 if depth electrode; 0 if subdural electrode). Intercept and patient were treated as random factors.

Likewise, the mixed model analysis determined whether cortical SPES via depth electrodes, compared to that via subdural electrodes, would elicit larger CCEPs and CCSRs.

2.13. Statistical analyses

Statistical analyses were performed using IBM SPSS Statistics version 22 (IBM Corp., Armonk, NY, USA) as well as Statistical and Machine Learning Toolbox MATLAB 2018b (The MathWorks Inc., Natick, MA, USA). The significance was set at a p-value of 0.05.

3. Results

3.1. Configurations and anatomical locations of implanted electrodes

We analyzed the empirical data from 14 patients who underwent SPES during extraoperative iEEG recording (Table 1). Bilateral sEEG recording was done with 115.7 [±12.8] analyzed depth electrodes per patient on average [standard error]. The subdural-depth combined recording was done with 113.8 [±3.9] analyzed subdural electrodes, and 8.4 [±1.1] analyzed depth electrodes per patient on average. The concordance of anatomical classification between two observers was substantial (Cohen's kappa = 0.78, $p < 0.001$). According to the consensus following group discussions, 86 depth electrodes were located at the deep white matter, 59 at the shallow white matter, 213 at the gray matter, 37 at the CSF space, and 89 outside the brain (Fig. 2; Videos S1 and S2).

SPES was delivered to a total of 120 depth electrode pairs (91 sEEG pairs). The cumulative number of CCEP/CCSR recording channels was 14,165.

3.2. CCSRs measured on bilateral and ipsilateral average montages on sEEG recording

Our empirical sEEG data indicated that ipsilateral average montage was more suitable to measure a near-field neuronal response to SPES compared to bilateral average montage. The Wilcoxon-Signed rank test showed that the CCSR amplitude outside the brain was larger on bilateral than ipsilateral average montage (Median difference: 28.0 μV; $p<0.01$). Based on the cluster-based permutation test, a large proportion of contacts outside the brain were suggested to show a significantly reproducible early CCSR component on bilateral average montage (54.2%) and ipsilateral average montage (49.7%). In other words, bilateral average montage was more unsuitable than ipsilateral average montage in our bilateral sEEG cohort.

3.3. Visual assessment of CCEPs and CCSRs measured on bipolar, Laplacian, and ipsilateral average montages

Our empirical sEEG data supported the notion that bipolar montage, compared to average montage, may be more suitable to measure a near-field neuronal response to SPES. Fig. 3 presents representative CCEPs measured on bilateral average montage, ipsilateral average montage, and bipolar montage. On bilateral and ipsilateral average montages, the amplitudes of an early negative response (also known as N1) at electrodes at the deep white matter (i.e., C1-C5) appeared larger than those at the gray matter (C6 and C10). Bipolar montage made the N1 CCEP amplitudes at the deep white matter contacts drastically reduced. Thus, large N1 CCEP responses at the white matter level, specifically seen on average montages, were suggested to be far-field potentials (Lachaux et al., 2003; Worrell et al., 2012; Kambara et al., 2018).

Fig. 4 presents another representative CCEPs and CCSRs measured on bipolar, ipsilateral average, and Laplacian montages. This figure supports the notion that bipolar and Laplacian montages, compared to ipsilateral average montage, may be more suitable to measure a near-field neuronal response to SPES. On ipsilateral average montage, a large N1 CCEP was noted at electrode contacts outside the brain (Fig. 4C). Conversely, bipolar (Fig. 4B) and Laplacian montages (Fig. 4D) made the N1 CCEP amplitude at contacts outside the brain drastically reduced.

Likewise, on ipsilateral average montage, early CCSRs were noted at contact outside the brain (Fig. 4F). Bipolar (Fig. 4E) and Laplacian montages (Fig. 4G) reduced the amplitude of early CCSRs at contacts outside the brain.

3.4. Quantitative assessment of CCEPs and CCSRs measured on bipolar, Laplacian, and ipsilateral average montages

Fig. 5 presents how well bipolar and Laplacian montages reduced the amplitude of CCEPs (Fig. 5A) and CCSRs (Fig. 5B) recorded at contacts outside the brain. Compare to those measured on ipsilateral average reference, the CCEP/CCSR amplitudes at contacts outside brain was 69-72% smaller on bipolar montage (CCEPs: 27.6% of that seen on average montage [95% CI: 23.5% to 31.7%]; CCSRs: 31.3% [95% CI: 28.7% to 34.0%]). Likewise, the CCEP/CCSR amplitudes at contacts outside brain was 77% smaller on Laplacian montage (CCEPs: 22.8% [95% CI: 18.9% to 26.6%]; CCSRs: 22.6% [95% CI: 20.6% to 24.6%]).

Conversely, the CCEP/CCSR amplitudes at the gray matter was well maintained on bipolar montage (CCEPs: 89.5% [95% CI: 85.5% to 93.6%]; CCSRs: 90.8% [95% CI: 88.8% to 92.9%]). The CCEP/CCSR amplitudes at the gray matter was 36-38% smaller on Laplacian montage compared to those measured on ipsilateral average montage (CCEPs: 62.2% [95% CI: 58.9% to 65.6%]; CCSRs: 63.5% [95% CI: 61.8% to 65.2%]).

As shown in Fig. 5, compared to those measured on ipsilateral average montage, the CCEP/CCSR amplitudes at the white matter was about 30-50% smaller on bipolar montage and 60-80% smaller on Laplacian montage.

3.5. The 3-step procedure optimally avoids the unwanted detection of CCSRs at contacts outside the brain

Fig. 6 indicates the thresholds optimally detecting CCSRs at gray matter contacts but not outside the brain. In our sEEG cohort of patients, the following 3-step procedure resulted in the successful detection of significant CCSRs specifically at the gray matter level. [Step A] iEEG must show a significantly reproducible amplitude augmentation based on the cluster-based permutation test (Maris and Oostenveld, 2007). [Step B] iEEG must show >80% augmentation of iEEG amplitude at 4-60 Hz at 11-50 ms. [Step C] The bipolar-to-average amplitude ratio must be >60%. In other words, iEEG must maintain at least 60% of amplitude on bipolar montage compared to that on ipsilateral average montage. With the aforementioned 3-step procedure employed, 5.3% of gray matter contacts turned out to show significant CCSRs on bipolar montage, whereas only 1.8% of the contacts outside the brain showed significant CCSRs. Likewise, with the 3-step procedure mentioned above, 2.6% of gray matter contacts turned out to show significant CCSRs on Laplacian montage, whereas 1.0% of the contacts outside the brain showed significant CCSRs.

Without the bipolar-to-average amplitude ratio-based threshold, 16.1% (Fig. 6A) of sEEG contacts ***outside the brain*** were suggested to show significant CCSRs. Employment of the bipolar-to-average amplitude ratio-based threshold of >30%, >60%, and >90% reduced the proportion of sEEG contacts outside the brain showing significant CCSRs to 3.7% (Fig. 6B), 1.8% (Fig. 6C), and 1.2% (Fig. 6D). Conversely, with the employment of the bipolar-to-average amplitude ratio-based threshold of >30%, >60%, and >90%, the proportion of ***gray matter*** contacts showing significant CCSRs was reduced from 6.4% (Fig. 6A) to 6.0% (Fig. 6B), 5.3% (Fig. 6C), and 4.0% (Fig. 6D), respectively. Thus, we considered the bipolar-to-average amplitude ratio-based threshold of >60% to be most reasonable for the detection of significant CCSRs in our sEEG cohort.

3.6. The similarity of the rank order of CCEP/CCSR amplitudes among different electrode montages

We found that the spatial distributions of CCEPs/CCSRs were extremely similar between bipolar and Laplacian montages but moderately similar between bipolar and ipsilateral average montages in our sEEG cohort. Figs. 7A and 7B demonstrate that the rank order of CCEP amplitudes across contacts was highly correlated between bipolar and Laplacian montages (mean Spearman's rho across patients: 0.88; $p<0.001$) but the degree of correlation between bipolar and ipsilateral average montage was moderate (mean Spearman's rho: 0.55; $p<0.001$).

Likewise, Figs. 7C and 7D show that the rank order of CCSR amplitudes was highly correlated between bipolar and Laplacian montages (mean Spearman's rho: 0.96; $p<0.001$) but the degree of correlation between bipolar and ipsilateral average montage was moderate (mean Spearman's rho: 0.61; $p<0.001$).

3.7. Effects of the SPES sites (white matter vs. gray matter) on the CCEP/CCSR amplitudes in our sEEG cohort

SPES of structures more proximal to the deep white matter, compared to the cortical surface, elicited larger CCEPs and CCSRs (Fig. 8). The mixed model analysis revealed that SPES to deep white matter contacts was associated with larger CCEP amplitudes (mixed model estimate: +13.3 μV; $p<0.001$; Table 2). Conversely, the hemisphere contralateral to the SPES sites (mixed model estimate: −21.6 μV; $p<0.001$) was independently associated with smaller CCEP amplitudes.

Likewise, SPES to deep white matter contacts was associated with larger CCSR amplitudes (mixed model estimate: +224.6 μV; $p<0.001$; Table 3). Conversely, the hemisphere contralateral to the SPES sites (mixed model estimate: −403.0 μV; $p<0.001$) was independently associated with smaller CCSR amplitudes.

SPES of two white matter contacts elicited significant CCSRs in 3.4% of contacts, whereas SPES of directly overlying gray matter contacts elicited significant CCSRs in 2.7% of contacts (Fig. 9).

3.8. Effects of the cortical SPES via different types of electrodes (depth vs. subdural) on the CCEP/CCSR amplitudes

The mixed model analysis revealed that cortical SPES via depth electrodes, compared to that via subdural electrodes, was associated with minimally larger CCEP amplitudes (mixed model estimate: +3.1 μV; $p=0.147$ [not significant]) but significantly larger CCSR amplitudes (mixed model estimate: +249.4 μV; $p<0.001$).

Cortical SPES via depth and subdural electrodes elicited significant CCSRs at 5.1% and 2.6% of contacts, respectively.

4. Discussion

4.1. A practical guide for the assessment of CCEPs/CCSRs on depth recording

The present study suggests that the application of multiple electrode montages, including either bipolar or Laplacian montage, may be appropriate for the analysis of SPES-related neuronal responses recorded on depth iEEG recording. We recommend the following 3-step procedure, in any order, in the diagnostic use of CCEPs/CCSRs.

[Step A] Confirmation of reproducibility. One needs to confirm that SPES-related iEEG signal deflections are reproducible across single-pulse stimuli. This procedure can be done using visual assessment or statistical analysis (Matsumoto et al., 2004; Maris and Oostenveld, 2007; Sugiura et al., 2020). The purpose is to minimize the risk to erroneously interpret a single excessively large-signal deflection (Kambara et al., 2018) as a significant SPES-related neuronal response. In the present study, we visually confirmed the reproducibility of CCEPs with visual assessment and that of CCSRs with a cluster-based permutation test (Maris and Oostenveld, 2007; Silverstein et al., 2020).

[Step B] Quantification of responses. One can quantify the magnitude of SPES-related neuronal responses, either using an averaging procedure (i.e., CCEP) or a time-frequency approach (i.e., CCSR). We assume that the CCEP/CCSR amplitude at 11-50 ms can reflect neuronal responses via a single axonal propagation (Matsumoto et al., 2017; Sugiura et al., 2020). Our recent study showed that the N1 CCEP amplitude was negatively correlated to the length of the single-axonal white matter pathway measured on diffusion-weighted imaging tractography (Silverstein et al., 2020).

[Step C] Identification of near-field potentials. A comparison of the size of a given iEEG signal deflection between average montage and bipolar montages allows us to estimate whether a given signal deflection is a near-field potential generated by the adjacent cortex receiving SPES-related neuronal propagation. We agree with the notion that one may treat an iEEG signal deflection discernible on average montage but disappearing on bipolar montage as a potential generated by a distant source (or sources) (Lachaux et al., 2003; Worrell et al., 2012; Kambara et al., 2018). We found that the employment of bipolar montage, as compared to average montage, reduced the size of SPES-related iEEG deflections at the majority of contacts outside the brain (Fig. 6). In other words, reproducible SPES-related signal deflections of which amplitude is well maintained on bipolar montage are likely to reflect near-field potentials from the adjacent cortex effectively connected from the stimulus site.

Our empirical sEEG data externally support the validity of the historical preference of bipolar montage in SPES studies using depth electrodes, as shown in the results of literature review (Supplementary Figure S1).

4.2. What is the single best electrode montage?

Each electrode montage has the pros and cons. We do not suggest one is better than the other in every aspect. Thus, we recommend the CCEP/CCSR assessment using multiple montages. The rank order of CCEP/CCSR amplitudes in a given patient was extremely similar between bipolar and Laplacian montages (Fig. 7); both montages are suitable to measure near-field responses generated by local structures receiving SPES-induced propagation. Unlike Laplacian or average montages, bipolar montage *per se* may not tell us which of a pair of contacts is responsible for a given neuronal response of interest. Laplacian montage does not allow us to measure neuronal responses at the end of depth electrodes accurately. The computation of Laplacian reference is different between the depth (based on two adjacent contacts) and subdural recordings (based on four adjacent contacts).

4.3. CCEPs or CCSRs?

Our study was not designed to determine whether CCEPs are more useful than CCSRs, or *vice versa,* for the depth electrode assessment of SPES-based effective connectivity. CCSRs measure the modulations of iEEG amplitudes phase-locked and unlocked to the SPES onset and are agnostic of the polarity of SPES-related neuronal responses (Crone et al., 2001; Sugiura et al., 2020). Conversely, CCEPs measure phase-locked neuronal responses alone (Figs. 3B-3D, 4B-4D, and 8B-8C). The location of a contact showing a reversal of phase of

CCEPs may help clinicians in localizing the boundary between gray and white matter, if the MRI-electrode coregistration image is unavailable.

4.4. Methodological considerations

We still don't know whether the significance thresholds optimally distinguishing contacts at the gray matter from those outside the brain in our sEEG cohort are universally applicable to different cohorts of patients. The sample size of our sEEG patients was small in the present study. We analyzed a total of 91 SPES stimulus trials recorded with a total of 347 sEEG electrodes derived from three patients. These patients took different combinations of oral antiepileptic drugs, each of which might have an impact on neuronal propagations (Ziemann et al., 1996; Chen et al., 1997).

Why did multiple electrode contacts outside the brain exhibit apparent sEEG signal deflections on average montage in the present study? We attribute this observation to several methodological issues, some of which may have been specific to our sEEG recording protocol. We suspect that the total number of depth electrode contacts may not have been large enough to make the average reference to be silent at a practical level. The present study computed the average reference voltage by excluding all of the iEEG signals within 3 cm from the midpoint of the SPES sites. sEEG and subdural iEEG recordings had different sampling density in different dimensions. Adjacent contacts within a given sEEG depth electrode may have shared neuronal responses with a common phase. In contrast, the phases of neuronal responses at different electrode sites may be more variable on subdural iEEG recording with a center-to-center electrode distance of 10 mm (Sugiura et al., 2020).

The present study does not clarify what area is the optimal location for the reference electrode. We did not assume that our system reference was utterly silent (Wennberg and Lozano, 2003; Mercier et al., 2017); thus, we re-referenced iEEG signals to the average reference (Crone et al., 2001; Lesser et al., 2010; Nariai et al., 2011). Conversely, some investigators treat an extra- or intra-cranial electrode distant from the SPES site as the original reference (Yamao et al., 2014; Shimada et al., 2017). The benefit of an extracranial reference electrode includes a smaller probability of the reference contaminated by SPES-related neuronal responses. In contrast, the limitation consists of higher susceptibility to movement-related artifacts. An intracranial or subgaleal electrode facing the bone may serve as a more resilient reference. However, even such an intracranial electrode is not entirely silent (Nune et al., 2011), and the placement of such a reference electrode would require additional skin incision.

4.5. Impact of the stimulation site on CCEPs/CCSRs

The present study demonstrated that subcortical SPES elicited significantly greater CCEP/CCSR amplitudes. The proportion of contacts showing significant CCSRs was 28% higher when contacts at the white matter were stimulated compared to at the gray matter. These observations are consistent with a previous SPES study using sEEG recordings that white matter stimulation has a higher probability (by 61%) to show CCEP-based effective connectivity than gray matter stimulation (Trebaul et al., 2018). Investigators previously suggested that white matter stimulation may directly activate neural fibers and elicit both

orthodromic and antidromic propagations to connected regions (Yamao et al., 2014; Enatsu et al., 2016; Trebaul et al., 2018). It is also plausible to hypothesize that some of the subcortical contacts may have been attached to the white matter fibers derived not only from the overlying cortex but also from the distant cortex.

Our novel findings include that intracortical stimulation via depth electrodes, compared to cortical stimulation using overlying subdural electrodes, elicited significantly greater CCSR amplitudes. Thereby, the intensity (5 mA) and pulse width (300 μs) remained constant across stimuli. Our observation can be attributed to the proximity between electrode contacts and white matter. It is also possible that structures between the cortex and subdural electrodes (e.g., pia mater) may have reduced or dispersed the excitatory effect of SPES on the cortex. Our findings might be useful for investigators who titrate the SPES intensity based on the neuronal responses observed on an individual basis. Our study suggests that depth electrodes, compared to subdural ones, may require less intensity of SPES to activate the underlying axons. Previous studies reported that 50-Hz electrical stimulation mapping with depth electrodes required about 2-mA smaller intensity to induce a clinical symptom compared to that with subdural electrodes (Zea Vera et al., 2017; Arya et al., 2020).

Supplementary Material

Refer to Web version on PubMed Central for supplementary material.

Acknowledgments

We are grateful to Karin Halsey, BS, REEGT. and Jamie MacDougall, RN, BSN, CPN at Children's Hospital of Michigan for the collaboration and assistance in performing the studies described above. This work was supported by NIH grant NS064033 (to E.A.) and JST CREST grant JPMJCR1784 (to T.M.).

Abbreviations

CCEPs	cortico-cortical evoked potentials
CCSRs	cortico-cortical spectral responses
CSF	cerebrospinal fluid
iEEG	intracranial electroencephalography
RMS	root mean square
sEEG	stereo-electroencephalography
SOZ	seizure onset zone
SPES	single-pulse electrical stimulation

References

Alarcón G, Martinez J, Kerai SV, Lacruz ME, Quiroga RQ, Selway RP, et al. In vivo neuronal firing patterns during human epileptiform discharges replicated by electrical stimulation. Clin Neurophysiol 2012;123(9):1736–44. 10.1016/j.clinph.2012.02.062. [PubMed: 22410162]

Arya R, Ervin B, Holloway T, Dudley J, Horn PS, Buroker J, et al. Electrical stimulation sensorimotor mapping with stereo-EEG. Clin Neurophysiol 2020 (in press). 10.1016/j.clinph.2020.04.159.

Asano E, Juhász C, Shah A, Sood S, Chugani HT. Role of subdural electrocorticography in prediction of long-term seizure outcome in epilepsy surgery. Brain 2009;132(4):1038–47. 10.1093/brain/awp025. [PubMed: 19286694]

Chen R, Samii A, Canos M, Wassermann EM, Hallett M. Effects of phenytoin on cortical excitability in humans. Neurology 1997;49(3):881–3. 10.1212/WNL.49.3.881. [PubMed: 9305361]

Cohen J A coefficient of agreement for nominal scales. Educ Psychol Measurement 1960;20(1):37–46. 10.1177/001316446002000104.

Crone NE, Boatman D, Gordon B, Hao L. Induced electrocorticographic gamma activity during auditory perception. Clin Neurophysiol 2001;112(4):565–82. 10.1016/S1388-2457(00)00545-9. [PubMed: 11275528]

Crowther LJ, Brunner P, Kapeller C, Guger C, Kamada K, Bunch ME, et al. A quantitative method for evaluating cortical responses to electrical stimulation. J Neurosci Methods 2019;311:67–75. 10.1016/j.jneumeth.2018.09.034. [PubMed: 30292823]

Cuello Oderiz C, von Ellenrieder N, Dubeau F, Eisenberg A, Gotman J, Hall J, et al. Association of cortical stimulation-induced seizure with surgical outcome in patients with focal drug-resistant epilepsy. JAMA Neurol 2019;76(9):1070–8. 10.1001/jamaneurol.2019.1464.

Delorme A, Makeig S. EEGLAB: an open source toolbox for analysis of single-trial EEG dynamics including independent component analysis. J Neurosci Methods 2004;134:9–21. 10.1016/j.jneumeth.2003.10.009. [PubMed: 15102499]

Enatsu R, Kanno A, Ohtaki S, Akiyama Y, Ochi S, Mikuni N. Intraoperative subcortical fiber mapping with subcortico-cortical evoked potentials. World Neurosurg 2016;86:478–83. 10.1016/j.wneu.2015.10.043. [PubMed: 26520432]

Gkogkidis CA, Wang X, Schubert T, Gierthmuhlen M, Kohler F, Schulze-Bonhage A, et al. Closed-loop interaction with the cerebral cortex using a novel micro-ECoG-based implant: the impact of beta vs. gamma stimulation frequencies on cortico-cortical spectral responses. Brain-Computer Interfaces 2017;4(4):214–24. 10.1080/2326263X.2017.1381829.

Isnard J, Taussig D, Bartolomei F, Bourdillon P, Catenoix H, Chassoux F, et al. French guidelines on stereoelectroencephalography (SEEG). Neurophysiol Clin 2018;48(1):5–13. 10.1016/j.neucli.2017.11.005. [PubMed: 29277357]

Kambara T, Sood S, Alqatan Z, Klingert C, Ratnam D, Hayakawa A, et al. Presurgical language mapping using event-related high-gamma activity: the Detroit procedure. Clin Neurophysiol 2018;129(1):145–54. 10.1016/j.clinph.2017.10.018. [PubMed: 29190521]

Koubeissi MZ, Lesser RP, Sinai A, Gaillard WD, Franaszczuk PJ, Crone NE. Connectivity between perisylvian and bilateral basal temporal cortices. Cereb Cortex 2012;22(4):918–25. 10.1093/cercor/bhr163. [PubMed: 21715651]

Kural MA, Tankisi H, Duez L, Sejer Hansen V, Udupi A, Wennberg R, et al. Optimized set of criteria for defining interictal epileptiform EEG discharges. Clin Neurophysiol 2020;131(9):2250–4. 10.1016/j.clinph.2020.06.026. [PubMed: 32731161]

Lachaux JP, Rudrauf D, Kahane P. Intracranial EEG and human brain mapping. J Physiol Paris 2003;97(4-6):613–28. 10.1016/j.jphysparis.2004.01.018. [PubMed: 15242670]

Lesser RP, Crone NE, Webber WRS. Subdural electrodes. Clin Neurophysiol 2010;121(9):1376–92. 10.1016/j.clinph.2010.04.037. [PubMed: 20573543]

Li G, Jiang S, Paraskevopoulou SE, Wang M, Xu Y, Wu Z, et al. Optimal referencing for stereo-electroencephalographic (SEEG) recordings. Neuroimage 2018;183:327–35. 10.1016/j.neuroimage.2018.08.020. [PubMed: 30121338]

Logothetis NK, Augath M, Murayama Y, Rauch A, Sultan F, Goense J, et al. The effects of electrical microstimulation on cortical signal propagation. Nat Neurosci 2010;13(10):1283–91. 10.1038/nn.2631. [PubMed: 20818384]

Maris E, Oostenveld R. Nonparametric statistical testing of EEG- and MEG-data. J Neurosci Methods 2007;164(1):177–90. 10.1016/j.jneumeth.2007.03.024. [PubMed: 17517438]

Matsumoto R, Nair DR, LaPresto E, Najm I, Bingaman W, Shibasaki H, et al. Functional connectivity in the human language system: a cortico-cortical evoked potential study. Brain 2004;127(10):2316–30. 10.1093/brain/awh246. [PubMed: 15269116]

Matsumoto R, Nair DR, LaPresto E, Bingaman W, Shibasaki H, Luders HO. Functional connectivity in human cortical motor system: a cortico-cortical evoked potential study. Brain 2007;130(1):181–97. 10.1093/brain/awl257. [PubMed: 17046857]

Matsumoto R, Kunieda T, Nair D. Single pulse electrical stimulation to probe functional and pathological connectivity in epilepsy. Seizure 2017;44:27–36. 10.1016/j.seizure.2016.11.003. [PubMed: 27939100]

Matsuzaki N, Juhasz C, Asano E. Cortico-cortical evoked potentials and stimulation-elicited gamma activity preferentially propagate from lower- to higher-order visual areas. Clin Neurophysiol 2013;124(7):1290–6. 10.1016/j.clinph.2013.02.007. [PubMed: 23523110]

Mercier MR, Bickel S, Megevand P, Groppe DM, Schroeder CE, Mehta AD, et al. Evaluation of cortical local field potential diffusion in stereotactic electroencephalography recordings: A glimpse on white matter signal. Neuroimage 2017;147:219–32. 10.1016/j.neuroimage.2016.08.037. [PubMed: 27554533]

Nakai Y, Jeong JW, Brown EC, Rothermel R, Kojima K, Kambara T, et al. Three- and four-dimensional mapping of speech and language in patients with epilepsy. Brain 2017;140(5):1351–70. 10.1093/brain/awx051. [PubMed: 28334963]

Nariai H, Nagasawa T, Juhász C, Sood S, Chugani HT, Asano E. Statistical mapping of ictal high-frequency oscillations in epileptic spasms. Epilepsia 2011;52(1):63–74. 10.1111/j.1528-1167.2010.02786.x. [PubMed: 21087245]

Nishida M, Korzeniewska A, Crone NE, Toyoda G, Nakai Y, Ofen N, et al. Brain network dynamics in the human articulatory loop. Clin Neurophysiol 2017;128(8):1473–87. 10.1016/j.clinph.2017.05.002. [PubMed: 28622530]

Nune G, Winawer J, Rauschecker AM, Dastjerdi M, Foster BL, Wandell B, et al. Problem of signal contamination in interhemispheric dual-sided subdural electrodes. Epilepsia 2011;52(11):e176–80. 10.1111/j.1528-1167.2011.03284.x. [PubMed: 21973215]

Oostenveld R, Fries P, Maris E, Schoffelen JM. FieldTrip: open source software for advanced analysis of MEG, EEG, and invasive electrophysiological data. Comput Intell Neurosci 2011;2011:156869 10.1155/2011/156869. [PubMed: 21253357]

Prime D, Woolfe M, Rowlands D, O'Keefe S, Dionisio S. Comparing connectivity metrics in cortico-cortical evoked potentials using synthetic cortical response patterns. J Neurosci Methods 2020a;334:108559 10.1016/j.jneumeth.2019.108559. [PubMed: 31927000]

Prime D, Woolfe M, O'Keefe S, Rowlands D, Dionisio S. Quantifying volume conducted potential using stimulation artefact in cortico-cortical evoked potentials. J Neurosci Methods 2020b;337:108639 10.1016/j.jneumeth.2020.108639. [PubMed: 32156547]

Shimada S, Kunii N, Kawai K, Matsuo T, Ishishita Y, Ibayashi K, et al. Impact of volume-conducted potential in interpretation of cortico-cortical evoked potential: detailed analysis of high-resolution electrocorticography using two mathematical approaches. Clin Neurophysiol 2017;128(4):549–57. 10.1016/j.clinph.2017.01.012. [PubMed: 28226289]

Shimamoto S, Waldman ZJ, Orosz I, Song I, Bragin A, Fried I, et al. Utilization of independent component analysis for accurate pathological ripple detection in intracranial EEG recordings recorded extra- and intra-operatively. Clin Neurophysiol 2018;129(1):296–307. 10.1016/j.clinph.2017.08.036. [PubMed: 29113719]

Silverstein BH, Asano E, Sugiura A, Sonoda M, Lee MH, Jeong JW. Dynamic tractography: integrating cortico-cortical evoked potentials and diffusion imaging. Neuroimage 2020;215:116763 10.1016/j.neuroimage.2020.116763. [PubMed: 32294537]

Stolk A, Griffin S, van der Meij R, Dewar C, Saez I, Lin JJ, et al. Integrated analysis of anatomical and electrophysiological human intracranial data. Nat Protoc 2018;13(7):1699–723. 10.1038/s41596-018-0009-6. [PubMed: 29988107]

Sugiura A, Silverstein BH, Jeong JW, Nakai Y, Sonoda M, Motoi H, et al. Four-dimensional map of direct effective connectivity from posterior visual areas. Neuroimage 2020;210:116548 10.1016/j.neuroimage.2020.116548. [PubMed: 31958582]

Swann NC, Cai W, Conner CR, Pieters TA, Claffey MP, George JS, et al. Roles for the pre-supplementary motor area and the right inferior frontal gyrus in stopping action: electrophysiological responses and functional and structural connectivity. NeuroImage 2012;59(3):2860–70. 10.1016/j.neuroimage.2011.09.049. [PubMed: 21979383]

Tallon-Baudry C, Bertrand O, Delpuech C, Permier J. Oscillatory gamma-band (30-70 Hz) activity induced by a visual search task in humans. J Neurosci 1997;17(2):722–34. 10.1523/JNEUROSCI.17-02-00722.1997. [PubMed: 8987794]

Tenke CE, Kayser J. Generator localization by current source density (CSD): implications of volume conduction and field closure at intracranial and scalp resolutions. Clin Neurophysiol 2012;123(12):2328–45. 10.1016/j.clinph.2012.06.005. [PubMed: 22796039]

Trebaul L, Deman P, Tuyisenge V, Jedynak M, Hugues E, Rudrauf D, et al. Probabilistic functional tractography of the human cortex revisited. Neuroimage 2018;181:414–29. 10.1016/j.neuroimage.2018.07.039. [PubMed: 30025851]

Usami K, Korzeniewska A, Matsumoto R, Kobayashi K, Hitomi T, Matsuhashi M, et al. The neural tides of sleep and consciousness revealed by single-pulse electrical brain stimulation. Sleep 2019;42(6):zsz050 10.1093/sleep/zsz050. [PubMed: 30794319]

Valentín A, Anderson M, Alarcón G, Seoane JJG, Selway R, Binnie CD, et al. Responses to single pulse electrical stimulation identify epileptogenesis in the human brain in vivo. Brain 2002;125(8):1709–18. 10.1093/brain/awf187. [PubMed: 12135963]

van 't Klooster MA, Zijlmans M, Leijten FS, Ferrier CH, van Putten MJ, Huiskamp GJ. Time-frequency analysis of single pulse electrical stimulation to assist delineation of epileptogenic cortex. Brain 2011;134(10):2855–66. 10.1093/brain/awr211. [PubMed: 21900209]

Wennberg RA, Lozano AM. Intracranial volume conduction of cortical spikes and sleep potentials recorded with deep brain stimulating electrodes. Clin Neurophysiol 2003;114(8):1403–18. 10.1016/S1388-2457(03)00152-4. [PubMed: 12888022]

Worrell GA, Jerbi K, Kobayashi K, Lina JM, Zelmann R, Le Van Quyen M. Recording and analysis techniques for high-frequency oscillations. Prog Neurobiol 2012;98(3):265–78. 10.1016/j.pneurobio.2012.02.006. [PubMed: 22420981]

Yamao Y, Matsumoto R, Kunieda T, Arakawa Y, Kobayashi K, Usami K, et al. Intraoperative dorsal language network mapping by using single-pulse electrical stimulation. Hum Brain Mapp 2014;35(9):4345–61. 10.1002/hbm.22479. [PubMed: 24615889]

Zea Vera A, Aungaroon G, Horn PS, Byars AW, Greiner HM, Tenney JR, et al. Language and motor function thresholds during pediatric extra-operative electrical cortical stimulation brain mapping. Clin Neurophysiol 2017;128(10):2087–93. 10.1016/j.clinph.2017.07.006. [PubMed: 28774583]

Ziemann U, Lönnecker S, Steinhoff BJ, Paulus W. Effects of antiepileptic drugs on motor cortex excitability in humans: a transcranial magnetic stimulation study. Ann Neurol 1996;40(3):367–78. 10.1002/ana.410400306. [PubMed: 8797526]

Zijlmans M, Jacobs J, Kahn YU, Zelmann R, Dubeau F, Gotman J. Ictal and interictal high frequency oscillations in patients with focal epilepsy. Clin Neurophysiol 2011;122(4):664–71. 10.1016/j.clinph.2010.09.021. [PubMed: 21030302]

Highlights

- We measured neuronal responses to single-pulse electrical stimulation (SPES).
- Bipolar and Laplacian montages record near-field responses on depth electrodes.
- Subcortical SPES elicited neuronal responses at large numbers of contacts.

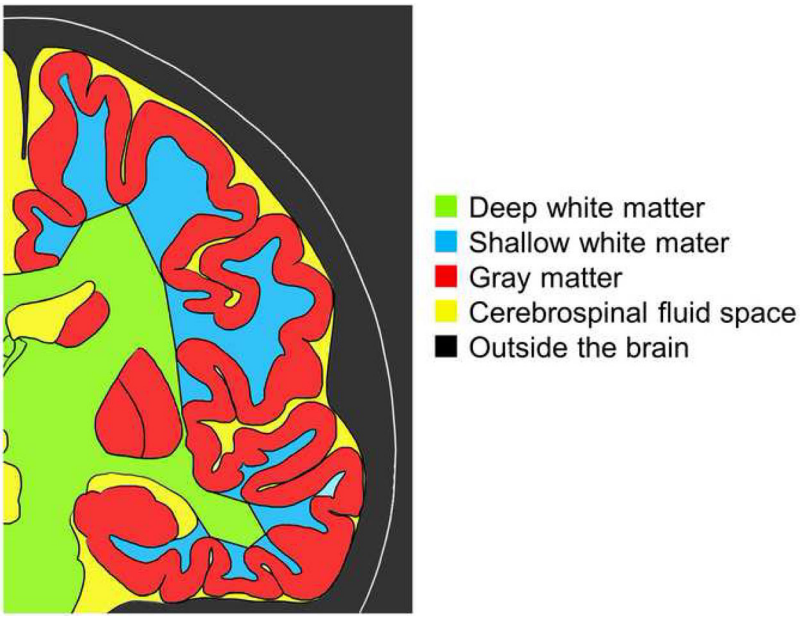

Fig. 1. Definition of brain regions.

A given depth contact was classified into one of the following anatomical categories: (a) deep white matter (light green), (b) shallow white matter (light blue), (c) gray matter (red), (d) cerebrospinal fluid space (yellow), and (e) outside the brain (black).

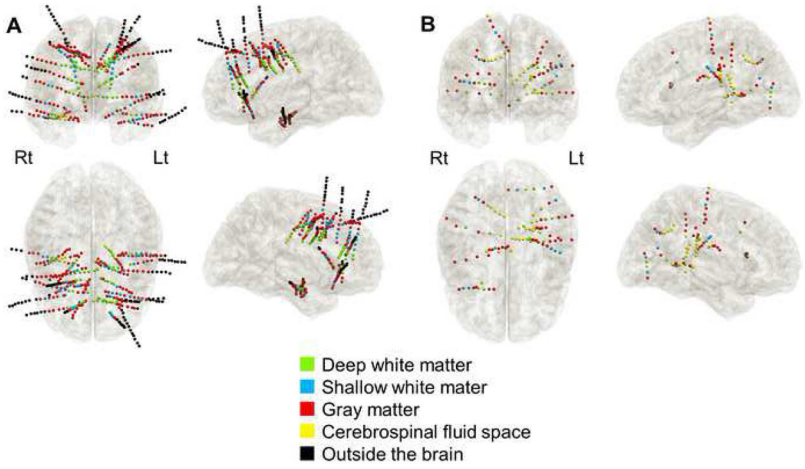

Fig. 2. The locations of depth electrode contacts.

(A) Depth electrodes placed stereotactically. (B) Those placed via craniotomy. Light green: deep white matter. Light blue: shallow white matter. Red: gray matter. Yellow: cerebrospinal fluid space. Black: outside the brain.

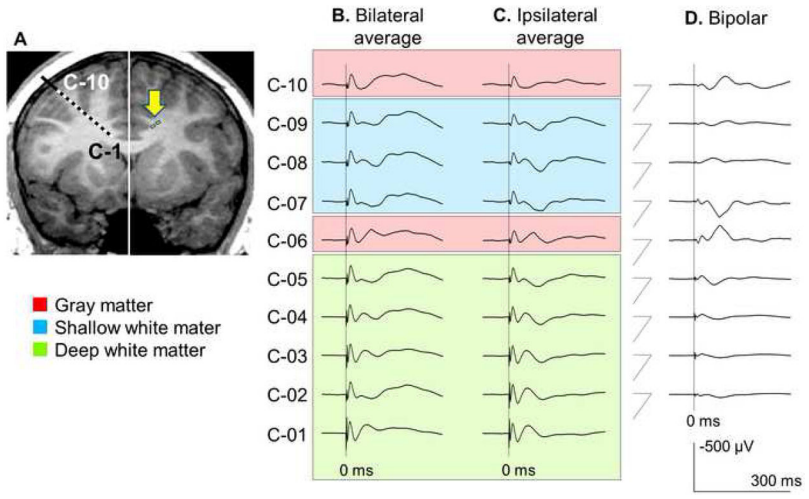

Fig. 3. Cortico-cortical evoked potentials (CCEPs) measured on different montages (patient #2).

(A) The yellow arrow denotes the stimulus pair. Electrode sites C1 to C10 recorded CCEPs. CCEPs measured on (B) bilateral average montage, (C) ipsilateral average montage, and (D) bipolar montage. Low-frequency filter: 0.016 Hz. High-frequency filter: 300 Hz.

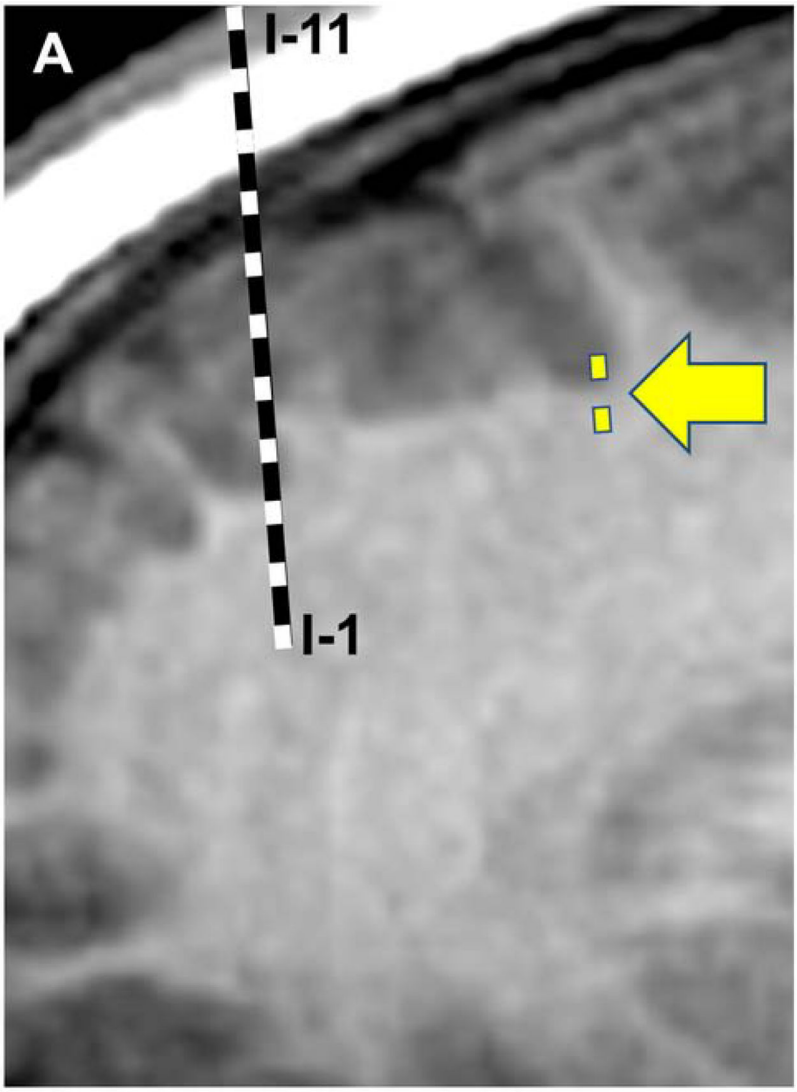

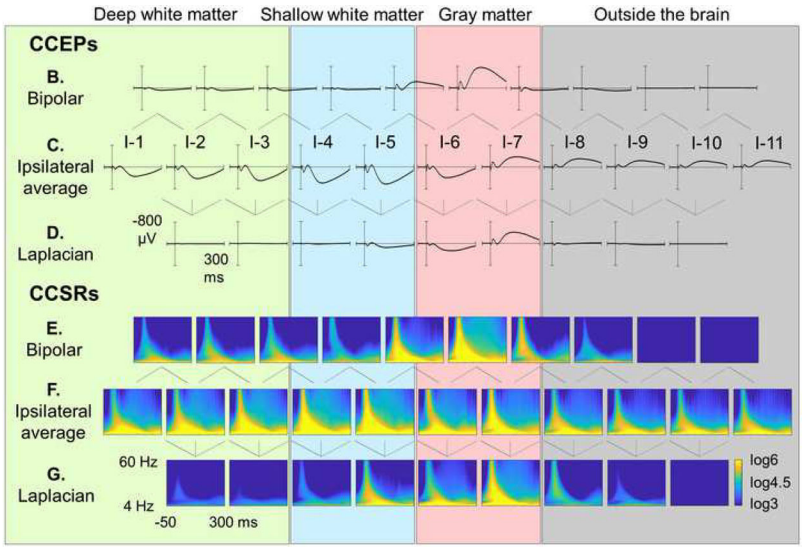

Fig. 4. Cortico-cortical evoked potentials (CCEPs) and cortico-cortical spectral responses (CCSRs) on different montages (patient #2).

(A) The yellow arrow suggests the stimulus pair to elicit CCEPs and CCSRs. Electrode sites I1 to I11 recorded CCEPs and CCSRs. CCEPs measured on (B) bipolar, (C) ipsilateral average, and (D) Laplacian montages. Low-frequency filter: 0.016 Hz. High-frequency filter: 300 Hz. CCSRs measured on (E) bipolar, (F) ipsilateral average, and (G) Laplacian montages.

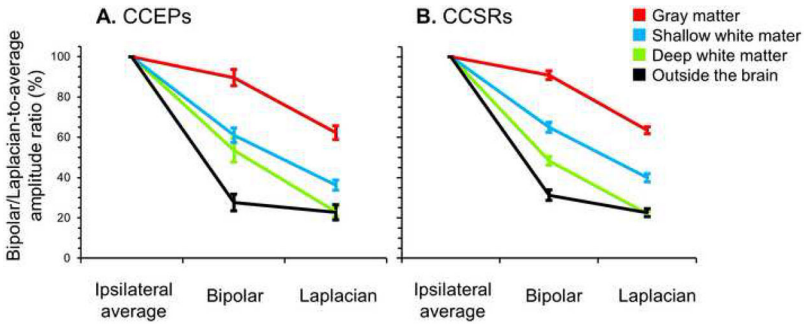

Fig. 5. Stereo-electroencephalography-based cortico-cortical evoked potential and spectral response (CCEP/CCSR) amplitudes on ipsilateral average reference, bipolar, and Laplacian montages.

(A) The mean relative N1 CCEP size (compared to that on ipsilateral average montage) at different anatomical levels is presented. Bar: 95% confidence interval. Electrode contacts outside the brain showed a relative CCEP size of 27.6% on bipolar montage; this indicates that the CCEP amplitude outside the brain was, on average, 72.4% smaller on bipolar montage compared to on ipsilateral average montage. (B) The mean relative CCSR size at different anatomical levels is likewise presented. Here, N1 size was defined as the square root of the mean of the squares of CCEP amplitude values from 11 to 50 ms.

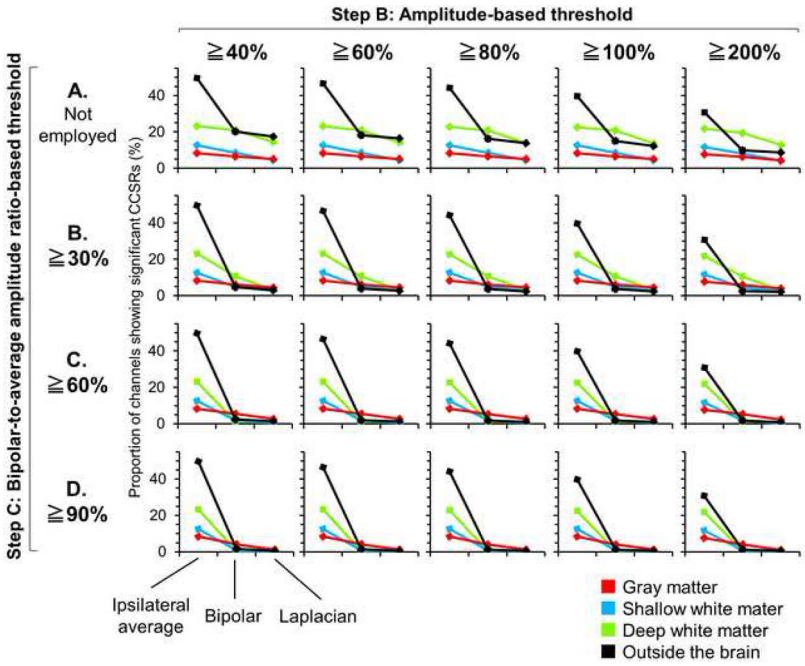

Fig. 6. The 3-step procedure to define significant cortico-cortical spectral responses (CCSRs) on stereo-electroencephalography depth recording.

The proportion of the number of electrode contacts showing significant CCSRs among all contacts at a given anatomical location (Black: outside the brain; Red: gray matter; Light blue: shallow white matter; Light green: Deep white matter). With different amplitude-based thresholds (>40%, >60%, >80%, >100%, >200% increase in amplitude) and bipolar-to-average amplitude ratio-based thresholds ([A] not employed, [B] >30%, [C] >60%, and [D] >90%), the proportion of contacts showing significant CCSRs was altered.

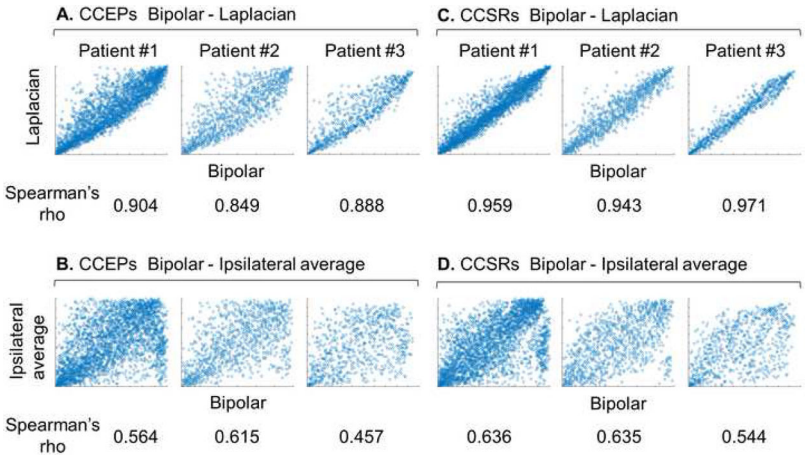

Fig. 7. The similarity of the rank order of cortico-cortical evoked potential (CCEP) and cortico-cortical spectral response (CCSR) amplitudes among different electrode montages.

Scatter plots of CCEP amplitude ranks (A) on bipolar and Laplacian montages and (B) on bipolar and ipsilateral average montages. Scatter plots of CCSR amplitude ranks (C) on bipolar and Laplacian montages and (D) on bipolar and ipsilateral average montages. The highest neuronal response within a given patient was given a rank of 1.

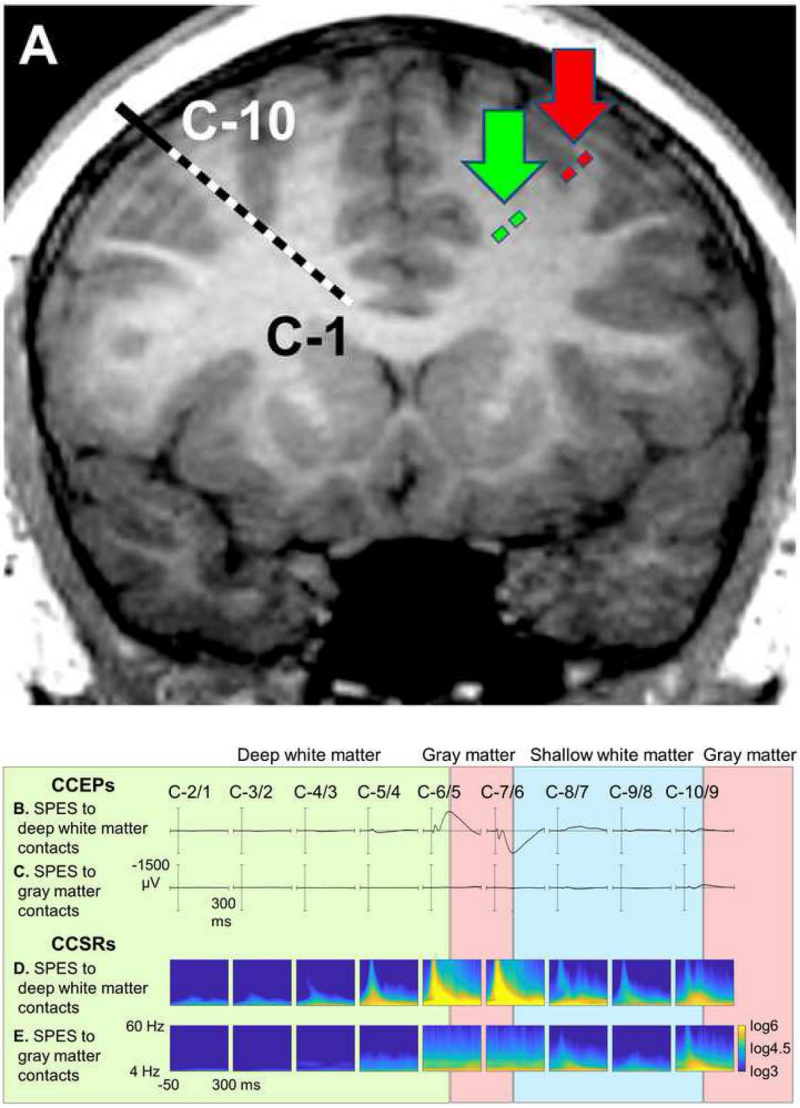

Fig. 8. Effects of single-pulse electrical stimulation (SPES) locations on the cortico-cortical evoked potential (CCEP) and cortico-cortical spectral response (CCSR) amplitudes (patient #2).

(A) Green arrow: SPES at the deep white matter. Red arrow: SPES at the gray matter. C1-C10: recording electrode sites. (B) CCEPs elicited by SPES at the deep white matter. Low-frequency filter: 0.016 Hz. High-frequency filter: 300 Hz. (C) CCEPs elicited by SPES at the gray matter. (D) CCSRs elicited by SPES at the deep white matter. (E) CCSRs elicited by SPES at the gray matter.

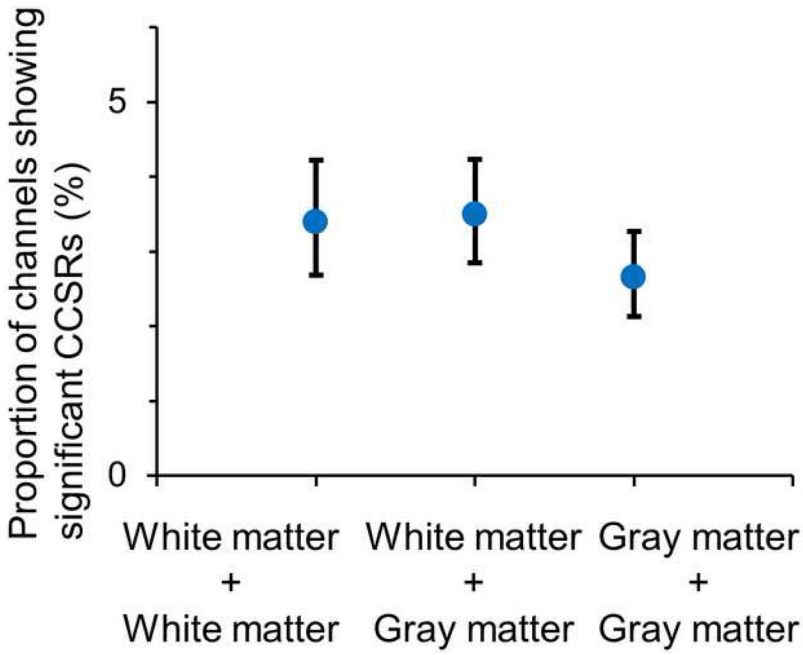

Fig. 9. Effects of single-pulse electrical stimulation (SPES) locations on the proportion of channels showing significant cortico-cortical spectral responses (CCSRs).

The proportion of electrode sites showing significant CCSRs elicited by SPES of different anatomical locations. Compared to SPES of a pair of gray matter contacts, that including a white matter contact elicited significant CCSRs more extensively (by 28-31%).

Table 1.

Patients profile.

Patient number	Age (years)	Gender	Sampled hemisphere	Number of included electrodes (depth/subdural)	Antiepileptic drugs	Age of epilepsy onset (years)	SOZ	Pathology
1	12	Male	Both	90 / 0	LTG, LAC	6	Both F	Not applicable
2	12	Female	Both	129 / 0	LEV, LAC, CLB	2	Lt F	Dysplasia
3	16	Female	Both	128 / 0	LEV, LTG, OXC	9	Rt F	Gliosis
4	2	Male	Right	8 / 125	LEV, OXC, CLB	0	F, P	Dysplasia
5	4	Female	Right	6 / 137	LAC	0	F, P	Dysplasia
6	8	Male	Left	13 / 99	LEV, OXC	6	P	Dysplasia
7	8	Female	Right	6 / 113	LAC, OXC, CLB	2.5	P	Gliosis
8	12	Male	Left	7 / 98	VPA, LEV	7	P	Dysplasia
9	13	Male	Left	11 / 96	LEV, LAC	10	O	Dysplasia
10	13	Male	Right	2 / 128	LEV, OXC	11	F	Dysplasia
11	16	Female	Left	15 / 110	OXC	7	P, T	Dysplasia
12	16	Female	Right	8 / 116	ZNS, LTG	6	P	Gliosis
13	17	Female	Left	8 / 114	LTG	15	T	Gliosis
14	19	Male	Right	8 / 116	LEV, OXC	0	O	Dysplasia

SOZ: Seizure onset zone. LTG: Lamotrigine. LAC: Lacosamide. LEV: Levetiracetam. CLB: Clobazam. OXC: Oxcarbazepine. VPA: Valproate. ZNS: Zonisamide. F: Frontal. P: Parietal. T: Temporal. O: Occipital.

Table 2.

Mixed model analysis to characterize the amplitude of cortico-cortical evoked potentials (CCEPs) elicited by stimulation of different regions.

Parameters	Estimate	S.E.	df	t	Pr(>|t|)	95% CI	
						L.L.	U.L.
(Intercept)	+0.0	5.3	9.8	0.001	0.999	−11.8	11.8
Deep white matter stimulation	+13.3	1.3	6343.8	10.352	**<0.001**	10.8	15.8
Shallow white matter stimulation	+10.9	1.3	7000.6	8.560	**<0.001**	8.4	13.4
Gray matter stimulation	+0.7	1.2	5241.6	0.568	0.570	−1.6	2.9
Recording with depth electrodes	+9.3	5.6	7.6	1.650	0.140	−3.8	22.5
Recording in the contralateral contacts	−21.6	1.3	8526.2	−17.155	**<0.001**	−24.0	−19.1

S.E.: Standard error. df: Degree of freedom. Pr: Probability. CI: Confidence interval. L.L.: Lower limit. U.L.: Upper limit. Each increase of a deep white matter contact was associated with an increase of the CCEP amplitude by 13.3 μV. Recording contacts contralateral to the SPES sites were independently associated with a smaller CCEP amplitude by 21.6 μV.

Table 3.

Mixed model analysis to characterize the amplitude of cortico-cortical spectral responses (CCSRs) elicited by stimulation of different regions.

Parameters	Estimate	S.E.	df	t	Pr(>|t|)	95% CI	
						L.L.	U.L.
(Intercept)	+412.5	162.9	10.8	2.532	0.028	53.2	771.8
Deep white matter stimulation	+224.6	27.8	8084.5	8.081	**<0.001**	170.1	279.1
Shallow white matter stimulation	+173.0	27.5	8255.1	6.288	**<0.001**	119.0	226.9
Gray matter stimulation	−13.6	25.2	7662.1	−0.538	0.590	−63.0	35.9
Recording with depth electrodes	−821.4	180.1	9.6	−4.560	**0.001**	−1225.2	−417.6
Recording in the contralateral contacts	−403.0	27.1	8527.6	−14.875	**<0.001**	−456.1	−349.9

S.E.: Standard error. df: Degree of freedom. Pr: Probability. CI: Confidence interval. L.L.: Lower limit. U.L.: Upper limit.